Improving the performance of high-laser-damage-threshold, multilayer dielectric pulse-compression gratings through low-temperature chemical cleaning

Heather P. Howard,* Anthony F. Aiello, Justin G. Dressler, Nicholas R. Edwards, Terrance J. Kessler, Alexei A. Kozlov, Ian R. T. Manwaring, Kenneth L. Marshall, James B. Oliver, Semyon Papernov, Amy L. Rigatti, Alycia N. Roux, Ansgar W. Schmid, Nicholas P. Slaney, Christopher C. Smith, Brittany N. Taylor, and Stephen D. Jacobs

Laboratory for Laser Energetics, University of Rochester, 250 East River Road, Rochester, New York 14623, USA

*Corresponding author: hhow@lle.rochester.edu

Received 20 November 2012; revised 7 February 2013; accepted 8 February 2013; posted 8 February 2013 (Doc. ID 180222); published 7 March 2013

A low-temperature chemical cleaning approach has been developed to improve the performance of multilayer dielectric pulse-compressor gratings for use in the OMEGA EP laser system. X-ray photoelectron spectroscopy results guided the selection of targeted cleaning steps to strip specific families of manufacturing residues without damaging the grating's fragile 3D profile. Grating coupons that were cleaned using the optimized method consistently met OMEGA EP requirements on diffraction efficiency and 1054 nm laser-damage resistance at 10 ps. The disappearance of laser-conditioning effects for the highest-damage-threshold samples suggests a transition from a contamination-driven laser-damage mechanism to defect-driven damage for well-cleaned components. © 2013 Optical Society of America

OCIS codes: 140.3330, 230.1950, 310.6845, 310.4925.

1. Introduction

Chirped-pulse amplification (CPA) has been an enabling technology in the development of ultrashort-pulse, high-power laser systems [1–5]. In a CPA setup, a pair of diffraction gratings is used to "chirp" the signal by stretching it in time, reducing the laser pulse to a much lower intensity before the beam travels through the amplifier. The amplified pulse passes through another set of gratings to recompress it to its original pulse duration. At the Laboratory for Laser Energetics (LLE), eight sets of tiled multilayer dielectric (MLD) gratings are used in pulse-compressor chambers for OMEGA EP's two short-pulse beamlines [6,7]. Each grating segment is 10 cm thick, 47 cm wide, and 43 cm tall; a complete tiled grating assembly includes three grating segments and is 1.4 m wide. The requirements on these critical large-aperture optics are rigorous: laser-induced damage thresholds (LIDTs) greater than 2.7 J/cm^2 (beam normal) for a 10 ps pulse at 1054 nm incident at 61° and a minimum diffraction efficiency (DE) of 97%. Because these demands have not yet been met, OMEGA EP's short-pulse beamlines are currently operated at ~60% of their design energy.

Surface contamination can dramatically reduce a grating's resistance to laser-induced damage [5,8–15]. OMEGA EP pulse compressor gratings are fabricated by etching a periodic groove structure (1740 lines/mm) into the top layer of a hafnia/silica multilayer mirror using interference lithography. Optionally, a bottom

1559-128X/13/081682-11$15.00/0

antireflective coating (BARC) is applied to the multilayer mirror to mitigate standing-wave effects during lithography and to improve fidelity. The grating fabrication process leaves large quantities of manufacturing residues and debris on the grating's surface that must be removed before the optic can go into service. Residues of hardened organic polymer BARC, in particular, are especially difficult to remove during final grating cleaning. Photoresist, BARC, etch residues, metal contaminants, surface debris, and light organic matter ultimately left on the grating can absorb energy during laser irradiation, initiating intense local heating and catastrophic laser-induced damage. Therefore, a final grating cleaning process that removes a broad spectrum of contaminant materials is essential. Mechanical contact with the delicate, microtextured grating surface must be absolutely avoided during cleaning, and cleaning techniques must not be so aggressive that they cause damage or defects. Additionally, short processing times and low temperatures are desirable for practical implementation on large parts and to mitigate thermal stress concerns.

2. MLD Grating Cleaning

Although surface contamination is a well-known cause of poor optical performance and laser-damage resistance, relatively few papers on cleaning methods for MLD gratings are available in the literature. Ashe *et al.* [11,12] were among the first to publish on this topic. They compared a number of chemical wet-cleaning methods commonly used in the semiconductor industry. Acid piranha, a mixture of sulfuric acid (H_2SO_4) and hydrogen peroxide (H_2O_2), was identified as the most promising chemistry for MLD grating cleaning based on postcleaning DE and LIDT results. Other groups [13–16] have also reported on the successful use of acid piranha to clean MLD gratings. Britten and Nguyen [15] developed a cleaning method for diffraction gratings that involved stripping bulk photoresist with an aqueous base and employing an oxidizing acid solution to remove residues, with oxygen plasma used as an intermediate step to remove fluorinated hydrocarbon residues. Plasma cleaning with oxygen and other gases has been suggested as a method for removing bulk organic layers of BARC [11,16] and photoresist [17,18] from gratings.

Nguyen *et al.* [19] and Britten *et al.* [20] demonstrated that briefly exposing an MLD grating to dilute buffered hydrofluoric acid (HF) solution could increase its resistance to laser damage. HF lightly etches the silica pillars, simultaneously removing embedded surface residues and reducing duty cycle (linewidth/period). Low-duty-cycle designs minimize electric field enhancement in the grating [21,22], but tall, narrow pillars can be difficult to fabricate using lithography. Chemical etchback allows for the surface profile to be adjusted as a final step in the manufacturing process. Britten *et al.* reported an average LIDT increase of 18.5% after etchback for 10 ps, 1053 nm damage testing at 76.5° incidence. The authors indicated that the HF linewidth-tailoring treatment "requires densified coating layers" [20] but did not elaborate.

While significant progress has been made in improving MLD grating cleaning processes in the past several years, no method has been shown to meet the in-vacuum OMEGA EP grating LIDT requirement of 2.7 J/cm^2 for a 1054 nm, 10 ps pulse incident at 61° on the final grating of a four-grating compressor. Thresholds exceeding 2.7 J/cm^2 have been reported for 10 ps testing [11,12,19,20,23,24], but in some of these studies the incidence angle was higher than 61° (necessitating a correction for comparison [25]), and in other cases damage-testing data were reported for only an air (or unspecified) environment. OMEGA EP gratings are operated in high vacuum. Testing environment can have a significant effect on laser-damage-threshold results, especially for nondensified, porous MLD coatings (such as those used by LLE) because humidity and the volatility of contaminant materials in the vacuum chamber can play important roles [8,26].

Another consideration is that the next generation of OMEGA EP gratings will, preferably, be fabricated with a BARC layer over the multilayer stack to minimize interference effects and distortion of the grating line structures at low duty cycles. Since many grating manufacturers do not use BARC, little information is available on stripping it from MLD gratings during final cleaning. Finally, wet cleaning of MLD gratings has typically been performed at high temperatures (60°C–110°C), especially when acid piranha is used to strip photoresist [11–14]. Such elevated processing temperatures have recently raised concerns about thermal-stress-induced defects, such as blistering and localized coating delamination, that can occur during cleaning. Hydrogen-peroxide-containing solutions are especially risky because H_2O_2 thermally decomposes and self-heats very rapidly at temperatures of 51°C and above, leading to sudden, uncontrolled increases in solution temperature [27]. Two examples of coating failure observed in our lab on hafnia/silica MLDs and MLD gratings following elevated-temperature cleaning are shown in Fig. 1. Figure 1(a) shows a group of ~40 μm diameter "blister" defects that nucleated near scratches on an MLD during piranha cleaning at 90°C. Figure 1(b) shows localized delamination of an MLD grating after piranha cleaning at 70°C. To compound concerns about thermal stresses, the behavior of small witness gratings may not be representative of full-scale pulse-compressor gratings. Large optics may be susceptible to modes of thermal-stress-induced failure not predicted by small witness parts [28].

To resolve the above issues, we sought a grating cleaning process that (1) meets OMEGA EP's specifications for DE and in-vacuum LIDT; (2) is compatible with standard, nondensified reactive-evaporation MLD coatings; (3) effectively strips both photoresist and BARC; and (4) requires no chemical processing at temperatures above 40°C (~20% below the critical temperature for self-heating of hydrogen peroxide) to reduce thermal-stress concerns.

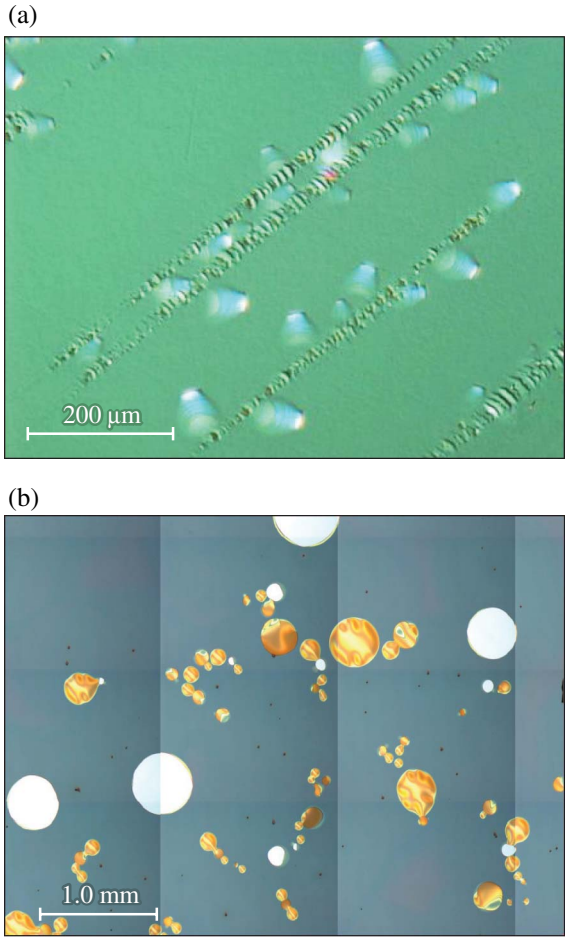

G9579J1

Fig. 1. (Color online) Coating failure observed after elevated-temperature acid piranha cleaning. (a) "Blister" defects observed on an MLD coating (no grating) after acid piranha cleaning at 90°C and (b) localized delamination observed on an MLD grating after acid piranha cleaning at 70°C.

3. Experimental

A. MLD Grating Samples

Cleaning experiments were performed on small-scale MLD grating coupons. Ten 100 mm diameter, 3 mm thick, round hafnia/silica MLD gratings were broken into eight equally sized, wedge-shaped coupons (80 samples total). The multilayer coating was a 4.8 μm thick modified quarter-wave thin film stack [29] with hafnia (HfO_2) and silica (SiO_2) used as the high- and low-index materials, respectively. The MLD was coated onto BK7 glass substrates by reactive evaporation at 200°C. Hafnia layers were deposited from a hafnium metal source using an oxygen backfill pressure of 2.0×10^{-4} Torr, while the silica layers were deposited from the oxide without an oxygen backfill (see [29] for a discussion of coating development for OMEGA EP gratings). A BARC layer was applied over the multilayer to mitigate interference effects during photolithography. Grooves (1740 lines/mm) were etched into the top silica layer of the MLD. The samples were "identical" in that they were produced in the same coating run and processed together up until the final cleaning stage. Except as noted, all cleaning experiments described in this article were performed on *uncleaned* gratings with BARC and photoresist still intact (that is, they were not subjected to any photoresist stripping or cleaning operations other than those described here). Uncleaned gratings had a characteristic brown, hazy film on their surface that could be readily identified visually. This brown coloration, attributed to a combination of photoresist, BARC, and/or fluorinated carbonaceous by-products formed during reactive ion etching of the groove structures, disappeared when a grating was well cleaned (see Fig. 2).

B. Measurement of Laser-Induced Damage Threshold and Diffraction Efficiency

Damage testing was performed at LLE's damage testing facility on the short-pulse (10 ps) system, which can be operated in both air and high-vacuum (4×10^{-7} Torr) environments. MLD grating samples were tested using *s*-polarized light at 1054 nm, using an incident beam angle of 61° and an irradiation spot size of 370 μm (e^{-1} in intensity) in the far field. Pulse fluence was measured during the test using an energy meter and a digital charge-coupled device situated in an optical plane equivalent to the sample plane. A commercial laser beam profiler (LBA-PC, Ophir-Spiricon) was used for beam analysis and fluence calculations. To minimize systematic error, the energy meter was recalibrated before each LIDT test. Laser-damage assessment was performed *in situ* using a white-light imaging system (~100× magnification). Damage was defined as a feature on the sample's surface that was not observed before laser irradiation. Image subtraction with background correction was used to assist the operator in identifying new features. The minimum detectable feature size was 2.7 μm. When switching between testing environments, samples were allowed to reach equilibrium with the environment (air or vacuum) for

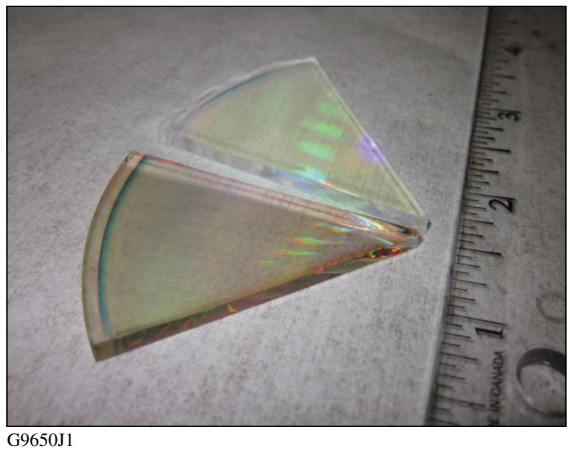
G9650J1

Fig. 2. (Color online) Grating wedge samples used in cleaning experiments, shown before (bottom) and after (top) cleaning. The ruler (right side), included for scale, is marked in inches.

Table 1. Treatments and Results for Acid Piranha Soak Cleaning Experiments at 40°C

Part ID	Ratio H_2SO_4:H_2O_2/Duration (min) Treatment 1	Treatment 2	Cleaning Temperature (°C)	Postcleaning DE (%)	Postcleaning LIDT (J/cm_2) in Vacuum 1-on-1	*N*-on-1
555-2	10:1/15	5:1/15	40	84.6 ± 0.8	0.66 ± 0.01	0.97 ± 0.03
555-1	5:1/15	2:1/15	40	91.7 ± 1.5	0.84 ± 0.06	1.08 ± 0.11
555-6	10:1/30		40	90.8 ± 1.2	0.76 ± 0.02	1.00 ± 0.05
555-5	5:1/30		40	81.3 ± 1.0	0.94 ± 0.05	1.04 ± 0.04
556-3	2:1/30		40	91.0 ± 1.6	0.95 ± 0.04	1.08 ± 0.06

24 h before testing continued. Damage thresholds are reported as beam normal fluences.

Each sample was tested in both 1-on-1 and *N*-on-1 testing regimes. See Wolfe *et al.* [30] for definitions of the 1-on-1 and *N*-on-1 tests, as well as two other well-known testing sequences not used in this work, *R*-on-1 and *S*-on-1. The 1-on-1 damage threshold is determined by irradiating a sample site with a single pulse and observing the sample for damage. This process is then repeated with increasing fluences on unirradiated sample sites until damage is observed. The 1-on-1 threshold is the average of the maximum fluence that did *not* result in damage and the minimum fluence that *did* result in damage. These fluences are required to be within 10% of each other; if they are not, testing continues with intermediate fluences until two sites can be identified with a fluence difference of less than 10%. The measurement error is taken as half the difference between the fluences for these two sites. The 1-on-1 testing sequence is performed once on each sample. *N*-on-1 (stepwise-ramped fluence) testing is conducted by irradiating the sample site at a fluence significantly below the 1-on-1 threshold for 10 shots. If no damage is detected, the fluence is increased slightly and the same site is irradiated with five more shots. If no damage is observed after these shots, fluence is increased again and another five shots are taken. This is continued until damage is observed in white light, at which point the damage onset fluence is recorded as the *N*-on-1 threshold for that site. The *N*-on-1 test is repeated for five sites on each MLD grating sample to generate an average and a standard deviation, which are reported as the *N*-on-1 threshold and measurement error, respectively.

The DE of each grating sample was measured with a 5 mm diameter beam incident at 72° on the sample surface (measurement uncertainty ±0.05%). Measurements were made in five locations on each part.

C. Acid Piranha Cleaning at Low Temperatures

Many of the techniques used to clean MLD gratings have been developed from methods used for wafer cleaning in the semiconductor industry. Acid piranha, for example, has been known as a photoresist stripper since at least 1975 [31], and its use is prevalent in the semiconductor industry. Standard operating procedure for acid piranha varies, but typical acid/peroxide ratios are in the range of 2:1–7:1 (two to seven parts 99% sulfuric acid to one part 30% hydrogen peroxide) and typical processing temperatures are in the range of 90°C–140°C [32,33]. Optimized piranha-cleaning processes for MLD gratings documented in the open literature have been consistent with these ranges [12–14]. Ashe *et al.* [12] found that laser-damage resistance was maximized when high cleaning temperatures were used and when the proportion of H_2O_2 in the piranha solution was high. Piranha 2:1 (two parts sulfuric acid, one part hydrogen peroxide) at 100°C gave the best LIDT results. The authors recorded *N*-on-1 damage thresholds as high as 3.27 J/cm^2 in air after piranha cleaning—exceeding the OMEGA EP pulse-compressor grating performance specification of 2.7 J/cm^2. Thresholds above 2.7 J/cm^2, however, were observed only for grating samples cleaned at temperatures of 80°C or higher, and all testing was done in air.

Because of thermal-stress concerns, we chose to work at temperatures of 40°C or below. Table 1 shows cleaning parameters and postcleaning DE and LIDT results for a group of grating samples cleaned for 30 min at 40°C in an acid piranha bath. Some experiments involved two piranha treatments. This

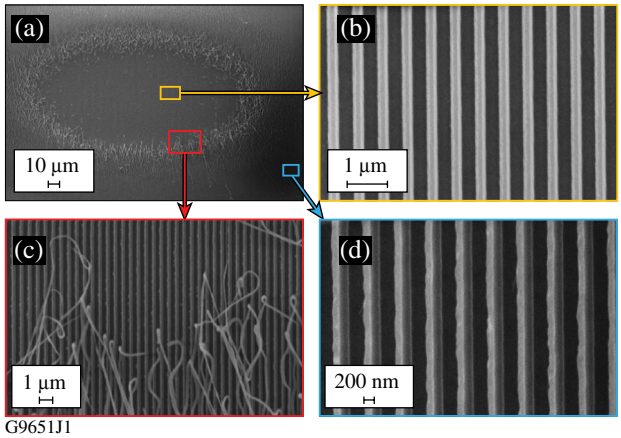

G9651J1

Fig. 3. (Color online) SEM images of a damage site on sample no. 555-5 irradiated at 1.40 J/cm^2 (1-on-1, 1054 nm, 10 ps, in vacuum, 61° incidence). (a) Entire damage site, (b) intact pillars at center of site where all photoresist was removed via laser irradiation ("cleaning" effect), (c) photoresist peeling away from pillars near the edge of the central region, and (d) grating pillars near the edge of the damage site, where the photoresist layer was tilted over and partially detached from the grating pillars due to the 61° incident angle of the laser beam.

Table 2. Optimized Cleaning Method

Process	Purpose	Method	Chemistry	Duration (min)	Temperature
1. Piranha strip [11–14,31–33]	Strips/softens photoresist and BARC	Spray onto optic; DI water rinse	H_2SO_4:H_2O_2 (5:1, 2:1)	5:1/15, 2:1/15	40°C–70°C
2. Plasma clean [15,17,18,32,33]	Removes light organics and partially removed material	Room air used as process gas	n/a	10	Room temperature
3. Ionic clean (SC-2) [32,33]	Eliminates remaining ionic/metallic contamination	Beaker soak; DI water rinse	HCl:H_2O_2:H_2O (1:1:6)	10	40°C–70°C
4. Plasma clean [15,17,18,32,33]	Removes light organics and partially removed material	Room air used as process gas	n/a	10	Room temperature
5. Oxide etch [20,32,33]	Removes a thin layer of SiO_2 along with any stubbornly adhered contaminants; thins pillars slightly, reducing duty cycle	Beaker soak; DI water rinse	HF:buffers (1:2500–1:3000)	5	Room temperature
6. Plasma clean [15,17,18,32,33]	Removes light organics and partially removed material	Room air used as process gas	n/a	10	Room temperature

methodology was motivated by Beck *et al.* [31], who suggested a two-step photoresist strip that employed first an acid-rich dehydrating bath, followed by a peroxide-rich oxidizing bath, to exploit the complementary material-removal mechanisms of acid piranha (dehydration and oxidation).

The experiments clearly demonstrated that at these low temperatures, acid piranha cleaning alone was inadequate. During damage testing, the unamplified laser beam used for alignment "wrote a track" onto the grating as it scanned across the samples, indicating that photoresist was not completely removed. Scanning electron microscope (SEM) observation of sample no. 555-5 (5:1 piranha, 30 min, 40°C) revealed intact photoresist all over the grating surface. In areas irradiated during damage testing, the photoresist had been deformed and/or stripped away, as shown in Fig. 3. The laser treatment provided a "cleaning" effect in the center of the damage site, where the photoresist was entirely removed by the incident laser beam. Near the edges of the region there was significant scatter from partially removed, deformed, and peeling strands of photoresist.

D. Targeted Chemical Cleaning

While acid piranha may be an effective solitary cleaning chemistry for MLD gratings at high temperatures, such was not our experience at 40°C. The intentionally low processing temperature necessitated a new approach. Because gratings are sensitive to surface pollutants of many different types, we developed a multistep technique to ensure broadband removal of performance-limiting contaminants. Cleaning techniques were adapted and combined from various sources to develop the optimized method detailed in Table 2. Drawn from semiconductor wafer processing and grating cleaning literature, the references describe other applications for each cleaning technique.

The cleaning process includes six major steps. First, acid piranha is used to strip photoresist, BARC, and carbonaceous etch residues. The piranha strip is followed by plasma cleaning in room air to clear away partially removed organic matter. Microscopic examination of samples suggested that BARC flakes off rather than gradually dissolving in piranha solution, and the plasma treatment ensures that material has been completely removed before proceeding to the next cleaning step. The third step in the cleaning process is an ionic clean with a standard clean 2 (SC-2) solution—a mixture of hydrochloric acid and hydrogen peroxide commonly used in the microelectronics industry to remove metallic contamination from silicon wafers. The inclusion of an ionic clean was motivated by the detection of molybdenum, a metal, on grating samples (see Section 3.E). The ionic clean is followed by a second plasma treatment to clear away light organic matter collected on the sample. The next step is an oxide etch, which reduces grating duty cycle and eliminates any remaining contaminants on the grating by removing a thin layer of silica [19]. The final step is a third air plasma treatment, which cleans the surface by removing light organics. Figure 4 compares SEM cross sections of a grating sample before and after cleaning, showing that the cleaning process removes BARC and photoresist layers from the pillar tops and narrows the grating pillars.

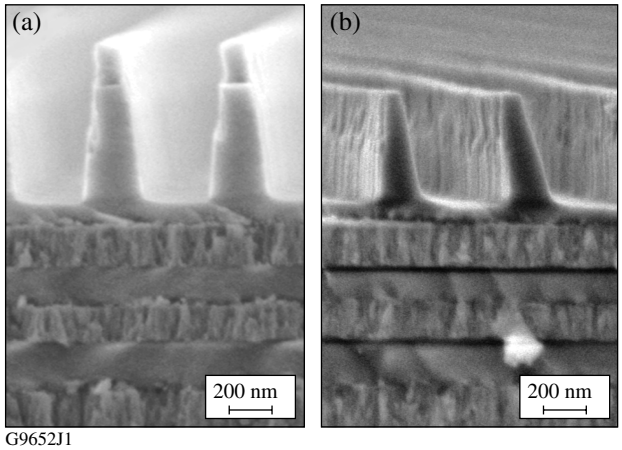

G9652J1

Fig. 4. SEM images showing MLD grating cross section (a) before chemical cleaning, with BARC and photoresist layers intact and (b) after cleaning, with BARC and photoresist stripped and grating pillars narrowed.

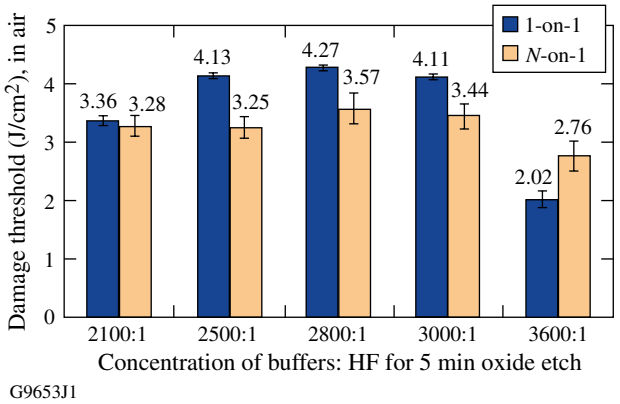

Fig. 5. (Color online) Effect of oxide etch concentration on laser-induced-damage threshold for a set of five MLD gratings cleaned according to the optimized method but with different buffered oxide etch/water ratios.

The optimized cleaning technique described above was developed through a series of experiments using the set of 80 identical grating samples described in Section 3.A. Damage thresholds were found to be especially sensitive to the dilution of HF acid used in the oxide etch step. Figure 5 shows the relationship between HF concentration and LIDT for a set of five MLD grating samples cleaned according to the method of Table 2 but with different ratios of buffered oxide etch to water used to prepare the oxide etch solution. Error bars show the 1-on-1 and N-on-1 LIDT measurement errors, as defined in Section 3.B. LIDT results were best for grating samples prepared using buffer:HF ratios in the range of 2500:1–3000:1 (between 2500 and 3000 parts water and buffers to every one part HF). An 1800:1 ratio (not shown) led to total delamination of the grating MLD during a 5 min etch.

The use of room air as the process gas in our plasma-cleaning setup is a unique aspect of the optimized grating cleaning process. Plasmas generated from oxygen gas (O_2) are more commonly used [15–18]. We found oxygen plasma to be overaggressive, however, and room air provided a gentler alternative. Figure 6 compares plasma-cleaning results for the two process gases. Eight grating samples were initially cleaned according to the method of Table 2 and then plasma cleaned for 1, 3, 5, or 10 min using either oxygen or room air as the process gas in a Harrick PDC-32G plasma cleaner. The plasma cleaner is a dedicated unit used only for grating-cleaning work and is equipped with a Pyrex chamber liner that is removed and cleaned with acetone between processes to mitigate contamination concerns. All samples treated with room-air plasma saw an increase in DE (average of +0.43%) and met the OMEGA EP specification of 97% after cleaning, while all samples treated with oxygen plasma saw a drop in DE (average of −0.63%), and only two of the four samples met the OMEGA EP specification. Shorter treatment times (15 and 30 s) were considered for oxygen plasma. The 15 s treatment improved DE modestly (+0.45%), but precise timing was a challenge for such

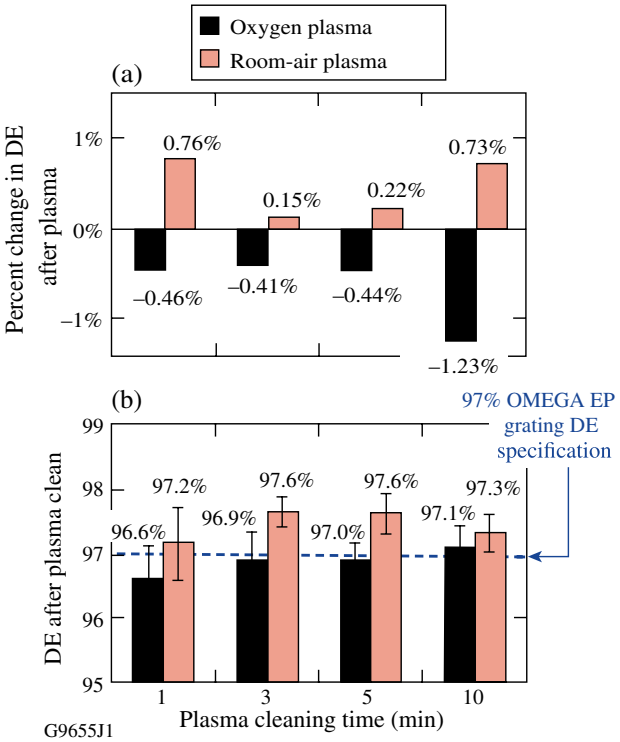

Fig. 6. (Color online) Comparison of oxygen and room-air plasma cleaning at room temperature. (a) Oxygen plasma cleaning for 1–10 min had a negative effect on DE, whereas room-air plasma cleaning enhanced DE. (b) All four samples treated with room-air plasma exceeded the 97% OMEGA EP grating DE specification, while only two of the four samples treated with oxygen plasma met this specification.

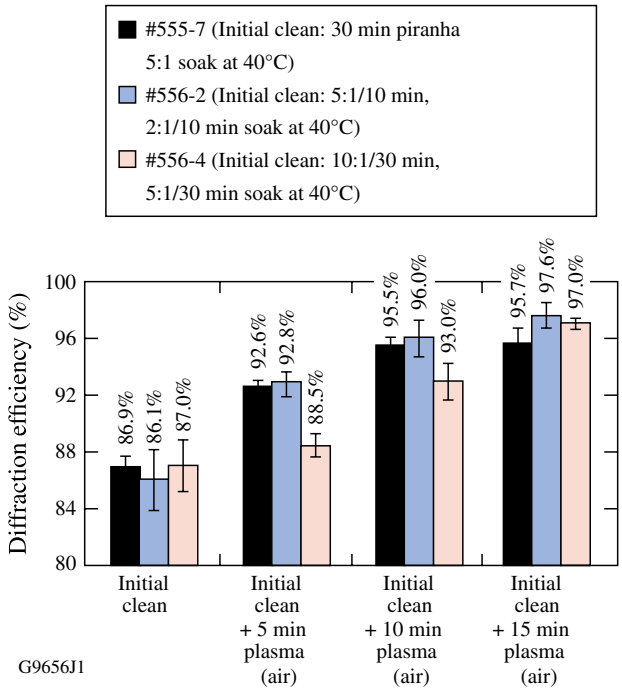

Fig. 7. (Color online) DE enhancement for a set of three MLD grating samples following a sequence of room-air plasma-cleaning treatments.

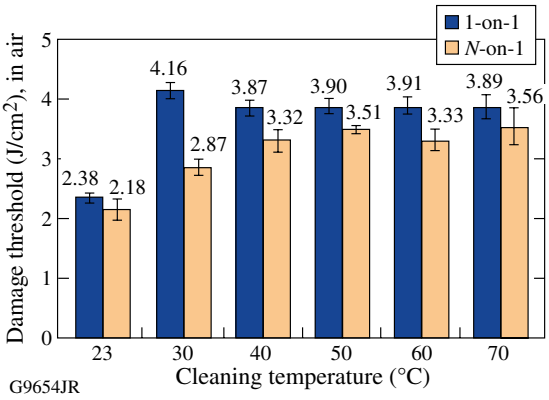

Fig. 8. (Color online) Relationship between in-air LIDT and cleaning temperature.

short process durations because initial adjustments to generate a stable plasma required several seconds. The 30 s treatment had a negative effect on DE (–0.39%). Because room-air plasma was gentler, cleaning times could be longer and process control was superior.

Room-air plasma was also found to be useful in "cleaning up" grating surfaces that failed to meet DE specifications after initial cleaning. Figure 7 shows the effect of sequential 5 min plasma-cleaning treatments on three piranha-cleaned samples having initially low diffraction efficiencies (86%–87%). After a 15 min total plasma treatment time, each sample had improved to >95% efficiency. We hypothesize that the air plasma treatment cleared away organic materials (BARC, photoresist, and/or carbonaceous etching by-products) that were softened or partially removed in previous cleaning steps. Air plasma cleaning is also effective at removing organic materials accumulated on the surface during storage and handling. In the optimized clean (Table 2), a plasma treatment is included after each wet-processing step to ensure that contaminants introduced (or partially removed) during previous cleaning steps are stripped away before moving on to the next cleaning phase.

A major advantage of the targeted cleaning approach is its effectiveness at low temperatures. Lower temperatures lessen concerns about thermal stresses and reduce susceptibility to blistering and delamination defects. Initial piranha-cleaning experiments at low temperatures had suggested that at temperatures 40°C and below, acid piranha alone could not remove BARC and photoresist from an MLD grating. The cleaning approach shown in Table 2 is much less temperature sensitive. Figure 8 shows in-air damage testing results for six samples cleaned using the optimized method at different cleaning temperatures. A one-way analysis of variances on the N-on-1 data showed that temperature had a significant effect on damage threshold (at significance level $\alpha = 0.05$) in the 23°C–70°C range. However, a second analysis limited to the range of 40°C–70°C showed that in this range, the effect of temperature was not statistically significant. These results suggest that cleaning temperatures can be safely reduced to the goal temperature of 40°C without negatively impacting grating performance.

E. X-Ray Photoelectron Spectroscopy Results

X-ray photoelectron spectroscopy (XPS) was used to evaluate the composition of materials on the grating surface at different phases in the cleaning process. Grating samples were prepared according to Table 2, with acid piranha and ionic cleaning steps performed at 70°C and an HF ratio of 3000:1. A piece of grating was reserved for XPS analysis after each process. XPS testing was performed by Penn State Materials Characterization Lab (sample no. 555-4), University of Dayton Research Institute (sample nos. 562-4A, 562-4B, 562-4C, and 562-4D), and Cornell Center for Materials Research (sample no. 555-5). Identically prepared samples were also submitted for laser-induced-damage testing. Results are listed in Table 3, and Fig. 9 plots the atomic percent of contaminants detected alongside the corresponding in-air LIDT results.

Since the top layer of the grating is SiO_2, the "ideal" XPS result for a well-cleaned grating would be 33% Si, 67% O, and nothing else. However, because samples are quickly contaminated with organic materials from the environment, some carbon is also expected. The detection of other elements (or large amounts of carbon) is undesirable and indicates insufficient removal of BARC, photoresist, and/or contaminants. In addition to silicon and oxygen (from the SiO_2 top layer), 42% carbon, 8% fluorine, and 3% molybdenum were detected on the uncleaned grating sample (no. 555-4).

Table 3. Elements Detected on MLD Gratings at Various Stages of Cleaning and Corresponding Damage Testing Results

Processing	Sample ID (XPS)	Elements Detected by XPS (at. %) O	Si	C	F	Mb	Hf	N	Sample ID (Damage Testing)	LIDT in Air (J/cm²) 1-on-1	N-on-1
Uncleaned	555-4	35.2	12.0	41.8	8.00	2.60	—	—	555-4	<0.13	
Piranha	562-4A	45.6	16.4	32.4	1.63	—	—	4.0	560-3	1.41 ± 0.06	1.87 ± 0.11
Piranha + plasma	562-4B	60.3	26.7	13.1	—	—	—	—	560-3	2.13 ± 0.11	2.27 ± 0.09
Piranha + plasma + ionic clean	562-4C	61.0	26.6	12.4	—	—	—	—	560-3	2.28 ± 0.05	2.45 ± 0.12
Piranha + plasma + ionic clean + plasma	562-4D	61.3	26.8	11.9	—	—	—	—	560-3	2.13 ± 0.04	2.34 ± 0.13
Piranha + plasma + ionic clean + plasma + oxide etch + plasma	555-5	60.1	23.8	14.2	—	—	1.0	1.0	555-5	4.11 ± 0.05	3.44 ± 0.21

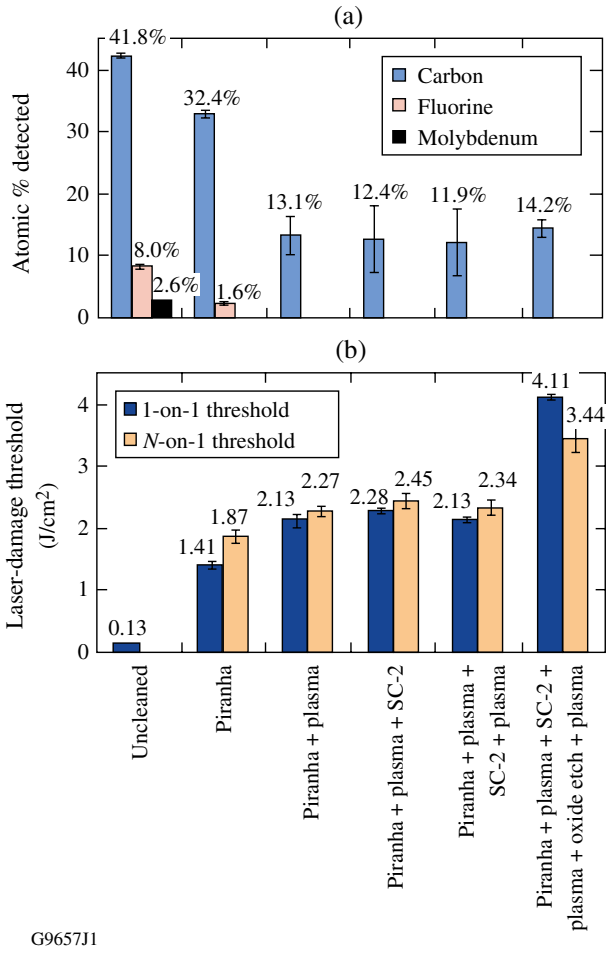

Fig. 9. (Color online) (a) Levels of carbon, fluorine, and molybdenum detected by XPS after each cleaning step and (b) corresponding in-air LIDT.

Carbon is attributed to organic photoresist/BARC layers, etch residues, and environmental contamination. Fluorine contamination most likely occurred from the production of fluorinated by-products during reactive-ion beam etching of the grating's groove structure, as has been reported by others [11,13,14]. The detection of molybdenum motivated the inclusion of a hydrochloric-acid-based ionic cleaning step to specifically target molybdenum and other trace metal contaminants. While not identified in XPS scans of our grating samples, Ashe *et al.* [11,12] detected potassium, sodium, chromium, iron, and aluminum ions on similarly prepared MLD grating samples using the more-sensitive time-of-flight secondary ion-mass spectrometry technique. Because metals absorb strongly at 1054 nm, damage resistance is quite sensitive to this type of contaminant.

After the piranha and plasma treatments, fluorine and molybdenum levels were below the XPS detection limit, and carbon levels had dropped to 13.1%. The biggest drop in carbon level occurred after the plasma treatment (rather than the piranha step), supporting our hypothesis that room-air plasma strips partially removed organic matter. The remaining cleaning steps (ionic clean, plasma, oxide etch, and plasma) had no significant effects on the XPS spectra. After bulk removal of photoresist and BARC, XPS may not be sensitive enough to identify trace contaminants that limit resistance to laser-induced damage.

F. Damage-Threshold and Diffraction-Efficiency Results

To investigate the consistency of grating performance, we assembled damage-threshold and diffraction-efficiency results for the set of samples cleaned using the optimized method. The samples included in this

Table 4. LIDT and DE Results for Grating Samples Cleaned using Optimized Method

Part ID	HF Dilution (HF:buffers)	Cleaning Temperature (Piranha Strip, Ionic Clean) [°C]	Postcleaning DE (%)	Postcleaning LIDT (J/cm²) in Air		Postcleaning LIDT (J/cm²) in Vacuum	
				1-on-1	*N*-on-1	1-on-1	*N*-on-1
562-6	2500:1	40	98.1 ± 0.4	4.40 ± 0.17	3.49 ± 0.17	3.30 ± 0.19	2.74 ± 0.14
566-1	2800:1	40	97.3 ± 0.4	3.87 ± 0.13	3.32 ± 0.18		
566-2[a]	2800:1	40	97.4 ± 0.5	3.32 ± 0.13	3.20 ± 0.12		
564-8[b]	2800:1	40	97.4 ± 0.2	4.24 ± 0.18	3.44 ± 0.21		
562-7	2500:1	50	97.4 ± 0.4	3.11 ± 0.10	3.19 ± 0.19	3.32 ± 0.02	2.69 ± 0.07
566-6	2800:1	50	97.4 ± 0.5	3.90 ± 0.12	3.51 ± 0.07		
557-2[c]	2800:1	50	96.4 ± 0.7	4.50 ± 0.08	3.55 ± 0.26	3.29 ± 0.10	2.66 ± 0.07
566-7	2800:1	60	97.5 ± 0.3	3.91 ± 0.15	3.33 ± 0.18		
555-5[c]	3000:1	60	97.0 ± 0.3	4.11 ± 0.05	3.44 ± 0.21		
564-7[a]	2500:1	70	98.7 ± 0.3	4.25 ± 0.16	3.54 ± 0.12		
564-6[b]	2500:1	70	97.6 ± 0.3	4.28 ± 0.20	3.06 ± 0.25		
562-3	2500:1	70	97.0 ± 0.3	4.07 ± 0.01	3.39 ± 0.10	3.19 ± 0.16	2.90 ± 0.04
566-8	2800:1	70	98.3 ± 0.5	3.89 ± 0.20	3.56 ± 0.31	3.70 ± 0.16	2.82 ± 0.20
555-2[c]	2800:1	70	97.8 ± 0.4	4.27 ± 0.05	3.57 ± 0.26		
Average (14 samples)			97.6	4.01	3.40	3.36	2.76
Standard deviation (14 samples)			0.55	0.40	0.16	0.20	0.10

[a]Piranha 2:1 only (30 min).
[b]Piranha 5:1 only (30 min).
[c]A reused grating sample was used for this experiment. The earlier cleaning experiment did not remove photoresist/BARC.

set were all cleaned according to the method of Table 2 or a minor variation thereof but were not processed identically. The optimized cleaning method includes a range of acceptable values for two of the cleaning parameters (processing temperature and HF concentration), and all samples that were within the ranges specified in Table 2 were included. We also extended the requirements for inclusion in the set to incorporate samples that were cleaned using 2:1 piranha or 5:1 piranha rather than our standard two-part piranha process. Data for the 14 samples meeting the above criteria, along with details of variations in cleaning methods used, are shown in Table 4.

The data show that the performance of samples cleaned using the optimized method was consistent, even with the minor differences in the processing details. Average in-air damage thresholds (1054 nm, 10 ps, 61° incidence) for the 14 samples tested in air were 4.01 J/cm^2 and 3.40 J/cm^2 in the 1-on-1 and N-on-1 regimes, respectively. For the five samples tested in a vacuum environment, average damage thresholds were 3.36 J/cm^2 (1-on-1) and 2.76 J/cm^2 (N-on-1). To our knowledge, this is the first time LIDTs exceeding the OMEGA EP requirement of 2.7 J/cm^2 in vacuum have been reported for MLD gratings. The average DE was 97.6%, meeting the OMEGA EP requirement on grating DE.

For all samples shown in Table 4, the 1-on-1 laser-damage threshold exceeded the N-on-1 threshold (with the exception of no. 562-7 in air testing). This result was surprising because in earlier experiments, N-on-1 thresholds were consistently higher than 1-on-1 thresholds [11,12]—a finding attributed to laser conditioning. During ramped-fluence testing, the laser "conditions" the grating in successive shots by removing near-surface absorbers at low, noncatastrophic fluences [5]. The beneficial effects of laser conditioning have been known for decades in the context of long-pulse (nanosecond) testing [30,34,35], but conditioning does not improve ultrashort-pulse laser-damage thresholds—in fact, multiple pulses have the opposite effect in subpicosecond testing because of the tendency for electronic defects to accumulate in the film with successive shots [36,37]. These disparate responses to conditioning are related to fundamental differences in damage mechanisms: short-pulse laser damage (<10 ps) is characterized by ablation, while long-pulse damage (>20 ps) is characterized by lattice heating and melting [36]. At transition pulse widths between these two regimes, multiple damage mechanisms may be at play. For 10 ps testing, Jovanovic *et al.* [5], Ashe *et al.* [11,12], and Kong *et al.* [24] demonstrated that laser-damage thresholds were higher when a ramped-fluence conditioning sequence was employed. In this work, however, samples cleaned using the optimized method (Table 4) showed no laser-conditioning effects at 10 ps. This suggests that in the case of well-cleaned gratings, N-on-1 thresholds were limited by the generation and buildup of electronic defects in the coating with successive laser shots, consistent with characteristic short-pulse damage behavior. We suspect that conditioning effects observed at 10 ps in our work (see, e.g., the data for partially cleaned samples in Table 3) and in other studies [5,11,12,24] may be contamination driven.

In general, the samples for which the 1-on-1 threshold exceeded the N-on-1 threshold were the best performers in terms of both DE and damage threshold. Figure 10(a) plots LIDT versus DE for the 80 samples cleaned as part of this study. N-on-1 damage thresholds are shown with light markers (orange online) and 1-on-1 thresholds are shown with dark markers (blue online); open markers indicate in-air data, while solid markers indicate vacuum data. If a sample improved with laser conditioning (N-on-1 LIDT > 1-on-1 LIDT), a round marker was used; if no conditioning effects were observed, a triangle marker was used. OMEGA EP specifications for DE and LIDT are marked on the plot. Nearly all samples that met both DE and LIDT requirements

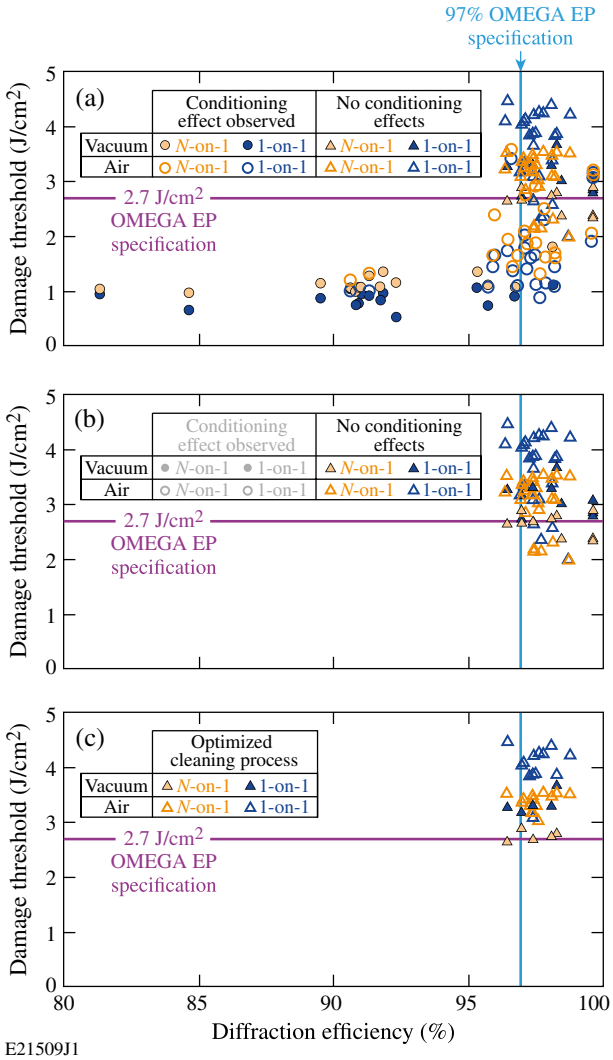

Fig. 10. (Color online) Damage threshold versus DE for (a) all samples, (b) only those samples showing no laser-conditioning effects (1-on-1 >N-on-1), and (c) only those samples cleaned using the optimized method (Table 2).

showed no laser-conditioning effect (triangle markers), while conditioning effects were observed for most of the poorly performing samples trailing off to the lower left-hand side of the scatter plot. Whether or not a sample exhibited a conditioning effect was an excellent predictor of its performance. Figure 10(b) limits the data of Fig. 10(a) to only those samples for which the 1-on-1 threshold exceeded the N-on-1 threshold. The majority of samples in this category meet both OMEGA EP requirements. Figure 10(c) further reduces the data set to only those samples cleaned using the optimized method, i.e., the 14 samples shown in Table 4. The minimum DE for this sample set was 96% and the minimum LIDT was 2.66 J/cm^2, illustrating that the cleaning technique enabled us to achieve consistently high DE and LIDT results.

4. Conclusions

A low-temperature cleaning method was developed to remove manufacturing residues from MLD pulse-compressor gratings manufactured with polymer BARC. The process, which is effective at processing temperatures as low as 40°, targets specific families of contaminants in a sequence of cleaning operations. Samples cleaned using the optimized method had outstanding performance: laser-induced-damage thresholds averaged 4.01 J/cm^2 in air and 3.36 J/cm^2 in vacuum (1-on-1 testing regime, 10 ps, 1054 nm, 61°), and average DE was 97.6%.

This work was supported by the U.S. Department of Energy Office of Inertial Confinement Fusion under Cooperative Agreement No. DE-FC52-08NA28302, the University of Rochester, and the New York State Energy Research and Development Authority. The support of DOE does not constitute an endorsement by DOE of the views expressed in this article.

References and Note

1. D. Strickland and G. Mourou, "Compression of amplified chirped optical pulses," Opt. Commun. **56**, 219–221 (1985).
2. G. A. Mourou, "Chirped pulse amplification," in *Encyclopedia of Modern Optics*, R. D. Guenther, D. G. Steel, and L. P. Bayvel eds., (Elsevier, 2005), pp. 83–84.
3. L. J. Waxer, D. N. Maywar, J. H. Kelly, T. J. Kessler, B. E. Kruschwitz, S. J. Loucks, R. L. McCrory, D. D. Meyerhofer, S. F. B. Morse, C. Stoeckl, and J. D. Zuegel, "High-energy petawatt capability for the OMEGA laser," Opt. Photonics News **16** (7), 30–36 (2005).
4. J. A. Britten, M. D. Perry, B. W. Shore, R. D. Boyd, G. E. Loomis, and R. Chow, "High-energy dielectric multilayer gratings optimized for manufacturability and laser damage threshold," Proc. SPIE **2714**, 511–520 (1996).
5. I. Jovanovic, C. G. Brown, B. C. Stuart, W. A. Molander, N. D. Nielsen, B. F. Wattellier, J. A. Britten, D. M. Pennington, and C. P. Barty, "Precision damage tests of multilayer dielectric gratings for high-energy petawatt lasers," Proc. SPIE **5647**, 34–42 (2005).
6. T. J. Kessler, J. Bunkenburg, H. Huang, A. Kozlov, and D. D. Meyerhofer, "Demonstration of coherent addition of multiple gratings for high-energy chirped-pulse-amplified lasers," Opt. Lett. **29**, 635–637 (2004).
7. J. Qiao, A. Kalb, M. J. Guardalben, G. King, D. Canning, and J. H. Kelly, "Large-aperture grating tiling by interferometry for petawatt chirped-pulse-amplification systems," Opt. Express **15**, 9562–9574 (2007).
8. B. Ashe, K. L. Marshall, D. Mastrosimone, and C. McAtee, "Minimizing contamination to multilayer dielectric diffraction gratings within a large vacuum system," Proc. SPIE **7069**, 706902 (2008).
9. W.-J. Kong, Z. C. Shen, J. Shen, J.-D. Shao, and Z.-X. Fan, "Investigation of laser-induced damage on multi-layer dielectric gratings," Chin. Phys. Lett. **22**, 1757–1760 (2005).
10. W. Kong, S. Liu, J. Shen, Z. Shen, J. Shao, Z. Fan, and J. Yao, "Study on LIDT of MDGs for different fabrication processes," Microelectron. Eng. **83**, 1426–1429 (2006).
11. B. Ashe, K. L. Marshall, C. Giacofei, A. L. Rigatti, T. J. Kessler, A. W. Schmid, J. B. Oliver, J. Keck, and A. Kozlov, "Evaluation of cleaning methods for multilayer diffraction gratings," Proc. SPIE **6403**, 64030O (2007).
12. B. Ashe, C. Giacofei, G. Myhre, and A. W. Schmid, "Optimizing a cleaning process for multilayer-dielectric- (MLD) diffraction grating," Proc. SPIE **6720**, 67200N (2007).
13. S. Chen, B. Sheng, K. Qui, Z. Liu, X. Xu, Y. Liu, Y. Hong, and F. Shaojun, "Cleaning multilayer dielectric pulse compressor gratings with top layer of HfO_2 by piranha solution," High Power Laser Particle Beams **23**, 2106–2110 (2011).
14. S. Chen, B. Sheng, X. Xu, and S. Fu, "Wet-cleaning of contaminants on the surface of multilayer dielectric pulse compressor gratings by the piranha solution," Proc. SPIE **7655**, 765522 (2010).
15. J. A. Britten and H. T. Nguyen, "Method for cleaning diffraction gratings," U.S. patent application 11/895,392 (23 August 2007).
16. B. Xu, S. D. Smith, D. J. Smith, and D. Chargin, "Reactive ion beam etching of large diffraction gratings," in *Proceedings of the 50th Annual Technical Conference of the Society of Vacuum Coaters* (Society of Vacuum Coaters, 2007), pp. 369–376.
17. Y. Hong, L. Liu, X. Zhou, X. Xu, and S. Fu, "Development of plasma photoresist descum system for large-aperture diffraction gratings," Vacuum **45**, 25–27 (2008).
18. A. Bodere, D. Carpentier, A. Accard, and B. Fernier, "Grating fabrication and characterization method for wafers up to 2-in," Mater. Sci. Eng. B **28**, 293–295 (1994).
19. H. T. Nguyen, C. C. Larson, and J. A. Britten, "Improvement of laser damage resistance and diffraction efficiency of multilayer dielectric diffraction gratings by HF etchback linewidth tailoring," Proc. SPIE **7842**, 78421H (2010).
20. J. Britten, C. Larson, M. D. Feit, and H. T. Nguyen, "Improvement of laser damage resistance and diffraction efficiency of multilayer dielectric diffraction gratings by HF-etchback linewidth tailoring," presented at the *ICUIL 2010 Conference*, Watkins Glen, New York, 26 September–1 October 2010, paper WO15.
21. N. Bonod and J. Néauport, "Optical performance and laser induced damage threshold improvement of diffraction gratings used as compressors in ultra high intensity lasers," Opt. Commun. **260**, 649–655 (2006).
22. J. Neauport, E. Lavastre, G. Razé, G. Dupuy, N. Bonod, M. Balas, G. de Villele, J. Flamand, S. Kaladgew, and F. Desserouer, "Effect of electric field on laser induced damage threshold of multilayer dielectric gratings," Opt. Express **15**, 12508–12522 (2007).
23. J. Keck, J. B. Oliver, T. J. Kessler, H. Huang, J. Barone, J. Hettrick, A. L. Rigatti, T. Hoover, K. L. Marshall, A. W. Schmid, A. Kozlov, and T. Z. Kosc, "Manufacture and development of multilayer diffraction gratings," Proc. SPIE **5991**, 59911G (2005).
24. F. Kong, Y. Jin, W. Chen, M. Zhu, T. Wang, D. Li, Z. Li, G. Xu, H. He, and J. Shao, "Effect of pulse duration on LIDT of multilayer dielectric gratings in vacuum," presented at SPIE Laser Damage Symposium 2012, Boulder, Colorado, 23–26 September 2012.
25. The OMEGA EP damage-threshold requirement is specified in a plane perpendicular to the beam incident at 61°; thresholds measured at other incidence angles cannot be directly compared. Higher incidence angles (Nguyen *et al.*'s data [19] were reported for 76.5° incidence, for example) correspond to larger on-sample beam areas, and therefore, higher

reported damage thresholds for the same beam fluence. For comparison, an approximate correction can be made using angular projection by multiplying the LIDT by the ratio of cosines of the incidence angles; e.g., an LIDT measured at 61° can be converted to 76.5° by multiplying by a factor of 2.07.
26. Y. Cui, Y. Zhao, H. Yu, H. He, and J. Shao, "Impact of organic contamination on laser-induced damage threshold of high reflectance coatings in vacuum," Appl. Surf. Sci. **254**, 5990–5993 (2008).
27. L.-K. Wu, K.-Y. Chen, S.-Y. Cheng, B.-S. Lee, and C.-M. Shu, "Thermal decomposition of hydrogen peroxide in the presence of sulfuric acid," J. Therm. Anal. Calorim. **93**, 115–120 (2008).
28. H. Howard, J. C. Lambropoulos, and S. Jacobs, "Dependence of thermal stresses on substrate thickness during wet processing of large coated optics," in *Optical Fabrication and Testing*, OSA Technical Digest (online) (Optical Society of America, 2012), paper OW3D.3.
29. J. B. Oliver, T. J. Kessler, H. Huang, J. Keck, A. L. Rigatti, A. W. Schmid, A. Kozlov, and T. Z. Kosc, "Thin-film design for multilayer diffraction gratings," Proc. SPIE **5991**, 59911A (2005).
30. C. R. Wolfe, M. R. Kozlowski, J. H. Campbell, F. Rainer, A. J. Morgan, and R. P. Gonzales, "Laser conditioning of optical thin films," Proc. SPIE **1438**, 360–375 (1990).
31. W. Beck, F. C. Brunner, P. U. Frasch, B. Ivancic, F. W. Schwerdt, and T. Vogtmann, "Method for stripping layers of organic material," U.S. patent 3,900,337 (19 August 1975).
32. G. W. Gale, R. J. Small, and K. A. Reinhardt, "Aqueous cleaning and surface conditioning processes," in *Handbook of Silicon Wafer Cleaning Technology*, K. A. Reinhardt and W. Kern, eds., 2nd ed., Materials Science & Process Technology Series (William Andrew, 2008), pp. 201–265.
33. D. W. Burns, "MEMS wet-etch processes and procedures," in *MEMS Materials and Processes Handbook*, R. Ghodssi and P. Lin, eds., (Springer, 2011), Chap. 8, pp. 457–665.
34. L. M. Sheehan, M. R. Kozlowski, F. Rainer, and M. C. Staggs, "Large-area conditioning of optics for high-power laser systems," Proc. SPIE **2114**, 559–568 (1994).
35. M. R. Kozlowski, M. Staggs, F. Rainer, and J. H. Stathis, "Laser conditioning and electronic defects of HfO_2 and SiO_2 thin films," Proc. SPIE **1441**, 269–282 (1991).
36. B. C. Stuart, M. D. Feit, S. Herman, A. M. Rubenchik, B. W. Shore, and M. D. Perry, "Optical ablation by high-power short-pulse lasers," J. Opt. Soc. Am. B **13**, 459–468 (1996).
37. M. Mero, B. Clapp, J. C. Jasapara, W. Rudolph, D. Ristau, K. Starke, J. Krüger, S. Martin, and W. Kautek, "On the damage behavior of dielectric films when illuminated with multiple femtosecond laser pulses," Opt. Eng. **44**, 051107 (2005).